Partial Channel State Information and Intersymbol Interference in Low Complexity UWB PPM Detection

Thomas Zasowski, Florian Troesch, and Armin Wittneben
Communication Technology Laboratory, ETH Zurich, 8092 Zurich, Switzerland
Email: {zasowski, troeschf, wittneben}@nari.ee.ethz.ch

Abstract— We consider an UWB PPM based wireless body area network with an average throughput of about 1Mbps. For a long battery autonomy a low duty cycle operation of the nodes and thus a high peak data rate is essential. Due to the moderate path loss a peak data rate in excess of 50 Mbps would be feasible within the FCC transmit power constraints. With current low complexity PPM detectors, such as the energy detector, the peak data rate is constrained to much lower values, because they are very sensitive to intersymbol interference (ISI). In this paper we constrain our attention to low complexity detectors for UWB PPM, which utilize an observation window of one symbol duration to generate the decision variables for the subsequent symbol decoder. The key contribution is a family of detectors, which utilize partial channel state information (CSI) to improve the robustness to ISI. Specifically we treat the following cases of partial CSI: (i) no CSI, (ii) average power delay profile (APDP), (iii) instantaneous power delay profile (IPDP). To further improve the performance in presence of ISI, a simple post-detection maximum-likelihood sequence estimator (MLSE) is introduced. Finally performance results are given, that highlight the tradeoff between complexity and performance covered by the proposed detection schemes.

I. INTRODUCTION

Ultra Wideband (UWB) body area networks (BAN) gained recently much interest [1] due to a bunch of attractive applications such as wireless health monitoring or ubiquitous computing. In a wireless body area network (WBAN), a number of small nodes are placed directly on the human body or close to it. Since WBAN nodes shall get their power from rechargeable batteries or by energy harvesting it is inevitable that the nodes are extremely energy efficient [2]. To meet such stringent energy requirements, a low duty cycle operation of the nodes and thus a high peak data rate is essential. Due to the moderate path loss in BANs [3], a peak data rate in excess of 50 Mbps would be feasible within the FCC transmit power constraints for a UWB system with a bandwidth of 500 MHz. However, the peak data rate is constrained to much lower values with current low complexity detectors, such as the energy detector, because this kind of receivers is very sensitive to intersymbol interference (ISI). In this paper we constrain our attention to low complexity detectors for UWB PPM, which utilize an observation window of one symbol duration to generate the

decision variables for the subsequent symbol decoder. Based on different levels of channel state information (CSI) the symbol-wise maximum likelihood (ML) detectors in presence of intersymbol interference are derived. We treat the cases that (i) no CSI, (ii) the average power delay profile (APDP), and (iii) the instantaneous power delay profile (IPDP) are available at the receiver. Besides these detectors, we also present the maximum likelihood detector with full CSI for reasons of comparison. Because the receiver complexity increases with a larger amount of CSI, we introduce a simple postdetection maximum likelihood sequence estimator (MLSE) that bases its decision on the output of an energy detector.

In [4], it is shown by means of a generalized maximum likelihood test that the energy detector is the optimum receiver for a 2PPM UWB system in the case of no CSI. Assuming the knowledge of the average power delay profile (APDP), the optimum receiver for 2PPM, resulting in an energy detector where the receive signal is weighted with the APDP, is derived in [5]. However, ISI is not considered in both ML derivations. The impact of ISI on PPM systems is investigated in [6] for the energy detector, the transmitted reference receiver and the rake receiver. A best and a worst case scenario are considered, i.e., orthogonal and almost fully overlapping PPM positions, respectively. However, only interference within one PPM frame is considered. The assumptions are chosen such that inter-frame interference (IFI) cannot occur. A performance degradation is observed for all three receivers in the presence of ISI.

The remainder of this paper is organized as follows. In Section II, the system model considered for the derivation of the ML detectors is introduced. The symbol-wise ML detectors assuming a different level of CSI are presented in Section III and the postdetecion MLSE in Section IV. Finally, the performance of the different ML detectors is evaluated in Section V and conclusions are given in Section VI.

II. SYSTEM MODEL

We consider an impulse radio (IR) UWB system with a binary pulse position modulation (2PPM). Moreover, it is assumed that only one pulse is transmitted per symbol, which
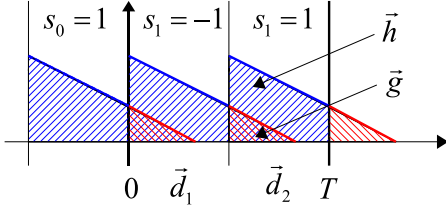
Fig. 1. Schematic of the considered receive signal positions

is reasonable for short range communication in wireless body area networks due to the moderate path loss. Although the symbol-wise ML detector bases its decision only on one single PPM frame, for the derivation, the previous receive signal has to be also taken into account as it may cause ISI as shown in Fig. 1. We assume in the remainder that the maximum duration of the channel impulse response is smaller than the duration of a PPM frame T, i.e., the ISI has only an impact on the next PPM half-frame. Time-hopping is omitted due to clarity of the derivation but can be easily included. Thus, the sampled receive signal in the considered PPM frame is given by

$$\vec{d_1} = \frac{1}{2}(1 - s_1)\vec{h} + \frac{1}{2}(1 + s_0)\vec{g} + \vec{n_1} \qquad (1)$$

for the first half frame and

$$\vec{d_2} = \frac{1}{2}(1 + s_1)\vec{h} + \frac{1}{2}(1 - s_1)\vec{g} + \vec{n_2} \qquad (2)$$

for the second half frame, depending on the transmit symbol $s_1 \in \{\pm 1\}$ in the present PPM frame and the transmit symbol $s_0 \in \{\pm 1\}$ in the previous PPM frame. $\vec{h}$ denotes the part of the channel impulse response (CIR) not causing ISI and $\vec{g}$ is the part of the CIR that causes ISI. Throughout the paper we assume that the taps of the CIR are statistically independent normal random variables with zero mean. $\vec{n_1}$ and $\vec{n_2}$ contain the additive white Gaussian noise (AWGN), both with variance σ^2. Since $\vec{d_1}$ and $\vec{d_2}$ are orthogonal in the time domain, the whole receive signal in the considered PPM frame can be described by

$$
\begin{aligned}
\vec{d} &= [\vec{d_1}, \vec{d_2}] \\
&= \frac{1}{2}[(1 - s_1)\vec{h_1} + (1 + s_0)\vec{g_1} \\
&\quad + (1 + s_1)\vec{h_2} + (1 - s_1)\vec{g_2}] + \vec{n}
\end{aligned} \qquad (3)
$$

with

$$
\begin{aligned}
\vec{h_1} &= [\vec{h}, 0, \ldots, 0] & \vec{h_2} &= [0, \ldots, 0, \vec{h}] \\
\vec{g_1} &= [\vec{g}, 0, \ldots, 0] & \vec{g_2} &= [0, \ldots, 0, \vec{g}]
\end{aligned} \qquad (4)
$$

and

$$\vec{n} = [\vec{n_1}, \vec{n_2}]. \qquad (5)$$

Both, $\vec{d_1}$ and $\vec{d_2}$ contain $N/2$ elements, i.e., $\vec{d}$ contains N elements.

III. SYMBOL-WISE MAXIMUM LIKELIHOOD DETECTOR

To derive the ML detector, we consider the probability $p(\vec{d}|s_1, s_0, \mathcal{C})$. There, $\mathcal{C}$ denotes the amount of channel state information that is available. Similar to [7], we assume the following cases of CSI for the derivation of the ML detectors: (i) full CSI, (ii) IPDP, (iii) APDP, and (iv) no CSI.

A. Full Channel State Information

If full CSI is available at the receiver side, i.e., $\mathcal{C}_{\text{full}} = [\vec{h}, \vec{g}]$, only the previous transmit symbol s_0 is unknown. Hence, s_0 has to be averaged out from the desired probability, i.e.,

$$p\left(\vec{d}|s_1 = s_i, \mathcal{C}_{\text{full}}\right) = \int_{-\infty}^{\infty} p(s_0)p\left(\vec{d}|s_1 = s_i, s_0, \vec{h}, \vec{g}\right) ds_0. \qquad (6)$$

In the remainder of the paper we assume equiprobable symbols such that $p(s_0) = \frac{1}{2}\delta(s_0 - 1) + \frac{1}{2}\delta(s_0 + 1)$ and $P[s_1 = 1] = P[s_1 = -1]$. Thus, the log-likelihood ratio is given by

$$L = \ln\left(\frac{p\left(\vec{d}|s_1 = 1, \mathcal{C}\right)}{p\left(\vec{d}|s_1 = -1, \mathcal{C}\right)}\right). \qquad (7)$$

In the case of full CSI, we obtain

$$
\begin{aligned}
L = &\frac{1}{2\sigma^2} \sum_{k=1}^{N/2} \left(2d_{k+N/2}h_k - 2d_k h_k + g_k^2 - 2d_{k+N/2}g_k\right) \\
&- \ln\left[\frac{\exp\left\{-\sum_{k=1}^{N/2}\frac{h_k g_k}{\sigma^2}\right\}\exp\left\{-\sum_{k=1}^{N/2}\frac{g_k^2 - 2d_k g_k}{2\sigma^2}\right\} + 1}{\exp\left\{-\sum_{k=1}^{N/2}\frac{g_k^2 - 2d_k g_k}{2\sigma^2}\right\} + 1}\right].
\end{aligned} \qquad (8)
$$

We refer to this receiver in the following as $\text{ML}_{\text{full,ISI}}$. If no ISI is present, the log-likelihood rule yields the matched filter receiver, i.e.,

$$L = \frac{1}{\sigma^2} \sum_{k=1}^{N/2} \left(d_{k+N/2}h_k - d_k h_k\right), \qquad (9)$$

where the receive signal is correlated with a template and thus the channel taps are coherently combined. This receiver is called in the remainder ML_{full}.

B. Instantaneous Power Delay Profile

In a next step, we assume that only the IPDP is available at the receiver side. We can write $\vec{h} = \vec{x} \odot \vec{z}$ and $\vec{g} = \vec{u} \odot \vec{v}$ where $\vec{x}$ and $\vec{u}$ denote the magnitudes of the channel impulse response (i.e. the IPDP) and $\vec{z}$ and $\vec{v}$ denote the signs of $\vec{h}$ and $\vec{g}$, respectively. Hence, the CSI is given by $\mathcal{C}_{\text{IPDP}} = [\vec{x}, \vec{u}]$. Since the signs z_k and v_k are equiprobable, the probability density functions are given by

$$
\begin{aligned}
p(z_k) &= \frac{1}{2}\delta(z_k - 1) + \frac{1}{2}\delta(z_k + 1) \\
p(v_k) &= \frac{1}{2}\delta(v_k - 1) + \frac{1}{2}\delta(v_k + 1).
\end{aligned} \qquad (10)
$$

The signs of the CIRs are unknown at the receiver side and have to be averaged out such that the desired probability depends only on the transmit symbol and the IPDP. This yields

$$p\left(\vec{d}|s_1 = s_i, \mathcal{C}_{\text{IPDP}}\right) = \prod_{k=1}^{N} \int_{-\infty}^{\infty} \int_{-\infty}^{\infty} \int_{-\infty}^{\infty}$$
$$p(s_0)p(z_k)p(v_k)p\left(d_k|s_1 = s_i, s_0, x_k, z_k, u_k, v_k\right) dv_k dz_k ds_0. \tag{11}$$

Evaluating (11) and inserting the obtained results into (7), we get for the log-likelihood ratio assuming knowledge of the IPDP

$$L = \sum_{k=1}^{N/2} \left(\ln \left[\exp\left\{ -\frac{u_k^2}{2\sigma^2} \right\} \right.\right.$$
$$\left(\cosh\left(\frac{d_{k+N/2}x_k + d_k u_k}{\sigma^2} \right) + \cosh\left(\frac{d_{k+N/2}x_k - d_k u_k}{\sigma^2} \right) \right)$$
$$\left.\left. + 2\cosh\left(\frac{d_{k+N/2}x_k}{\sigma^2} \right) \right] \right)$$
$$- \sum_{k=1}^{N/2} \left(\ln \left[\exp\left\{ -\frac{u_k^2}{2\sigma^2} \right\} \right.\right.$$
$$\left(\cosh\left(\frac{d_k x_k + d_{k+N/2} u_k}{\sigma^2} \right) + \cosh\left(\frac{d_k x_k - d_{k+N/2} u_k}{\sigma^2} \right) \right)$$
$$+ \exp\left\{ -\frac{u_k^2 - d_k x_k}{\sigma^2} \right\} \cosh\left(\frac{(d_{k+N/2} + d_k - x_k)u_k}{\sigma^2} \right)$$
$$\left.\left. + \exp\left\{ -\frac{u_k^2 + d_k x_k}{\sigma^2} \right\} \cosh\left(\frac{(d_{k+N/2} + d_k + x_k)u_k}{\sigma^2} \right) \right] \right). \tag{12}$$

Without ISI (i.e. $\vec{u} = 0$), the log-likelihood ratio (12) reduces

$$L = \sum_{k=1}^{N/2} \left(\ln \left[\cosh\left(\frac{d_{k+N/2}x_k}{\sigma^2} \right) \right] - \ln \left[\cosh\left(\frac{d_k x_k}{\sigma^2} \right) \right] \right), \tag{13}$$

i.e. the receive signal is weighted with the magnitude of the corresponding channel tap. The receiver with consideration of the ISI is denoted in the rest of the paper as $\text{ML}_{\text{IPDP,ISI}}$ while the latter one is referred to as ML_{IPDP}.

C. Average Power Delay Profile

In this case the receiver knows the correlation matrices of $\vec{h}$ and $\vec{g}$

$$\Lambda_{hh} = \begin{bmatrix} \mathcal{E}[h_1^2] & \cdots & 0 \\ \vdots & \ddots & \vdots \\ 0 & \cdots & \mathcal{E}[h_{N/2}^2] \end{bmatrix} = \begin{bmatrix} \lambda_{h1} & \cdots & 0 \\ \vdots & \ddots & \vdots \\ 0 & \cdots & \lambda_{hN/2} \end{bmatrix} \tag{14}$$

and

$$\Lambda_{gg} = \begin{bmatrix} \mathcal{E}[g_1^2] & \cdots & 0 \\ \vdots & \ddots & \vdots \\ 0 & \cdots & \mathcal{E}[g_{N/2}^2] \end{bmatrix} = \begin{bmatrix} \lambda_{g1} & \cdots & 0 \\ \vdots & \ddots & \vdots \\ 0 & \cdots & \lambda_{gN/2} \end{bmatrix}. \tag{15}$$

We rearrange the receive vector such that the kth tap of $\vec{d}_1$ and $\vec{d}_2$ are adjacent, i.e.,

$$\vec{d} = \left[d_1, d_{N/2+1}, d_2, d_{N/2+2}, \ldots, d_{N/2-1}, d_N \right]. \tag{16}$$

Using (16), we calculate the correlation matrix of the receive signal Λ_{dd}. According to [8], the desired probability assuming the knowledge of the correlation matrix Λ_{dd} is defined as

$$p\left(\vec{d}|s_1 = s_i, s_0, \Lambda_{dd}\right)$$
$$= \left(\frac{1}{\sqrt{2\pi}} \right)^N \frac{1}{\sqrt{\Delta_{dd}}} \exp\left(-\frac{1}{2} \vec{d}^T \Lambda_{dd}^{-1} \vec{d} \right) \tag{17}$$

where Δ_{dd} denotes the determinant of Λ_{dd} and $\vec{d}^T$ is the transpose of $\vec{d}$. After calculation of the determinant and the inverse of Λ_{dd} and after averaging over s_0, we obtain the log-likelihood ratio for $\text{ML}_{\text{APDP,ISI}}$

$$L = \sum_{k=1}^{N/2} \ln \left(\frac{1}{\sqrt{\zeta_k}} \exp\left\{ -\frac{d_k^2 \alpha_k + d_{k+N/2}^2 \beta_k}{2\zeta_k} \right\} \right.$$
$$\left. + \frac{1}{\sqrt{\sigma^2 \alpha_k}} \exp\left\{ -\frac{1}{2} \left(\frac{d_k^2}{\sigma^2} + \frac{d_{k+N/2}^2}{\alpha_k} \right) \right\} \right)$$
$$- \sum_{k=1}^{N/2} \ln \left(\frac{1}{\sqrt{\zeta_k}} \exp\left\{ -\frac{d_k^2 \beta_k + d_{k+N/2}^2 \alpha_k}{2\zeta_k} \right\} \right.$$
$$+ \frac{1}{\sqrt{\zeta_k + \lambda_{gk}\sigma^2}}$$
$$\left. \cdot \exp\left\{ -\frac{d_k^2 \beta_k + d_{k+N/2}^2(\beta_k + \lambda_{hk}) - 2d_k d_{k+N/2}\lambda_{gk}}{2\left(\zeta_k + \lambda_{gk}\sigma^2\right)} \right\} \right) \tag{18}$$

with $\alpha_k = \lambda_{hk} + \sigma^2$, $\beta_k = \lambda_{gk} + \sigma^2$, and $\zeta_k = \alpha_k \beta_k$.

In the case where no ISI is present, i.e., $\lambda_{gk} = 0$, we get the ML_{APDP} where the log-likelihood ratio is given by

$$L = \frac{1}{2\sigma^2} \sum_{k=1}^{N/2} \frac{d_{k+N/2}^2 - d_k^2}{1 + \frac{\sigma^2}{\lambda_{hk}}}. \tag{19}$$

This is a typical energy detector whose output is weighted with the APDP. This log-likelihood ratio without ISI corresponds to the result presented in [5].

D. No Channel State Information

Finally, we consider the case that the receiver only knows the average energy of the CIR. Due to the lack of additional CSI, the receiver assumes a uniform power delay profile in $\vec{h}$ and $\vec{g}$, i.e., $\lambda_h^2 = \sigma_h^2$ and $\lambda_g^2 = \sigma_g^2$. Thus, the probability density functions of the channel taps h_k and g_k follow as

$$p(h_k) = \frac{1}{\sqrt{2\pi\sigma_h^2}} \exp\left\{ -\frac{h_k^2}{2\sigma_h^2} \right\} \tag{20}$$

and

$$p(g_k) = \frac{1}{\sqrt{2\pi\sigma_g^2}} \exp\left\{ -\frac{g_k^2}{2\sigma_g^2} \right\}. \tag{21}$$

Similar to (11), the probability density function depending on s_1 only is given by

$$p\left(\vec{d}|s_1 = s_i\right) = \prod_{k=1}^{N} \int_{-\infty}^{\infty} \int_{-\infty}^{\infty} \int_{-\infty}^{\infty}$$
$$p(s_0)p(h_k)p(g_k)p\left(d_k|s_1 = s_i, s_0, h_k, g_k\right) dg_k dh_k ds_0. \quad (22)$$

After some calculations, we get for the log-likelihood ratio

$$L = \frac{1}{\xi} \sum_{k=1}^{N/2} \left(d_{k+N/2}^2 - d_k^2\right) + \ln\left[\left(\sqrt{\gamma} + \sqrt{2\sigma_g^2}\right)^{N/2}\right]$$
$$- \sum_{k=1}^{N/2} \left(\ln\left[\exp\left\{d_{k+N/2}^2 \gamma\right\} + \left(\frac{\xi\sqrt{2\nu}}{\sqrt{\xi - 2\nu}}\right)\right.\right.$$
$$\left.\left. \cdot \exp\left\{\frac{(4d_{k+N/2}\nu + d_k)^2}{\xi - 2\nu} + d_{k+N/2}^2 \nu - \frac{d_k^2}{\xi}\right\}\right]\right). \quad (23)$$

with $\xi = \frac{1}{2\sigma_h^2} - 1$, $\gamma = \frac{\sigma_g^2 \sigma^2}{\sigma_g^2 + \sigma^2}$ and $\nu = \frac{\sigma_g^2 \sigma^2}{2\sigma_g^2 + \sigma^2}$. The first sum in (23) corresponds to an energy detector while the remaining terms mitigate the impact of the ISI. Without ISI, i.e., $\sigma_g^2 = 0$, (23) yields the common energy detector [9], which we refer to as ED in the following.

IV. POSTDETECTION MAXIMUM LIKELIHOOD SEQUENCE ESTIMATOR

In the previous sections we considered symbol-wise ML detectors, which utilize different levels of CSI. They trade off receiver complexity and performance. The proposed detectors estimate each transmit symbol on the basis of an observation of the received signal in the corresponding PPM symbol frame. The robustness to ISI is improved by considering it in the symbol decision metric. In this section we follow an alternate approach. The simple symbol-wise ML detector for the "no CSI and no ISI" case (i.e. the energy detector) is combined with a two-state postdetection Maximum Likelihood Sequence Estimator (MLSE). As can be concluded from (23) with $\sigma_g^2 = 0$, for each iteration the branch metric of this MLSE involves two decision variables: the received energy in the first and second PPM half-frame of the respective symbol.

MLSE is a well-known technique to mitigate ISI. In the area of optical communications a lot of work on trellis encoders and MLSE for nonlinear amplitude detection receivers can be found. As for UWB-IR PPM in [10] and [11] the MLSE for a linear receiver front end is derived. In [12], decision feedback equalizers for UWB-IR on-off keying systems are considered. [13] investigates convolutional codes and Viterbi decoders for non-linear UWB-IR detection, where access to the receive signal is still possible.

The proposed MLSE works on the sample sequence at the output of the energy detector. In each PPM half-frame one sample $y_s = \sum_{k=(s-1)N/2+1}^{N/2} d_k^2$ is obtained. Let K be the number of 2PPM symbols. Then the sample sequence contains $2K + 1$ elements; two for each PPM frame and one trailing

sample to collect all energy of the last PPM symbol. We denote this sequence by the row vector

$$\vec{y} = [y_1, y_2, \ldots, y_{2K+1}]$$

We consider two variants of the MLSE. The first MLSE utilizes the channel state information C1 defined by the (4x4) matrix

$$\mathcal{C}_1 = \left[\begin{array}{cc} \vec{h}\vec{h}^T & \vec{h}\vec{g}^T \\ \vec{g}\vec{h}^T & \vec{g}\vec{g}^T \end{array}\right]. \quad (24)$$

This $\mathcal{C}_1$ can be measured with only a few pilot symbols. The number of pilot symbols can be further decreased by neglecting the off-diagonal elements, i.e.,

$$\mathcal{C}_2 = \vec{v}^T \vec{v} = \left[\begin{array}{cc} \vec{h}\vec{h}^T & 0 \\ 0 & \vec{g}\vec{g}^T \end{array}\right], \quad (25)$$

This is the CSI $\mathcal{C}_2$ of the second MLSE. This simplified MLSE assumes that $\vec{h}$ and $\vec{g}$ are orthogonal vectors.

Let s be the half-frame index (i.e. $s = 2k$ and $s = 2k + 1$ relate to the first and second PPM half-frame of the kth transmit symbol). We define a (2Kx1) vector $\vec{x}$, which identifies the PPM half-frames, that contain transmit pulses (i.e. $(x_{2k}, x_{2k+1}) = (1, 0)$ or $(0, 1)$ depending on the transmit symbol). The MLSE picks the vector $\hat{\vec{x}}$ which maximizes the probability that $\vec{y}$ was received given a certain CSI $\mathcal{C}_i$ and $\hat{\vec{x}}$ [14]:

$$\underset{\hat{\vec{x}}}{\operatorname{argmax}} \ p\left(\vec{y}|\hat{\vec{x}}, \mathcal{C}_i\right). \quad (26)$$

Due to the square and integrate device of the energy detector, the elements of the receive vector $\vec{y}$ are not Gaussian. If N is large, the law of large numbers [15] motivates the approximation of the elements of $\vec{y}$ as Gaussian random variables, i.e, we have:

$$\begin{aligned} y_s &= \vec{h}\vec{h}^T x_s + \vec{g}\vec{g}^T x_{s-1} + 2\vec{g}\vec{h}^T x_s x_{s-1} \\ &\quad + 2\vec{h}\vec{n}_s^T x_s + 2\vec{g}\vec{n}_s^T x_{s-1} + \vec{n}_s \vec{n}_s^T \\ &\approx s_s + z_s, \end{aligned} \quad (27)$$

where s_s is the signal component and z_s is a real Gaussian random variable with expectation $\overline{z}_s$ and variance $\sigma_{z,s}$ [16]:

$$\overline{z}_s = N\sigma^2 \quad (28)$$
$$\sigma_{z,s}^2 = 2N\sigma^4 + 4(\vec{h}\vec{h}^T x_s + \vec{g}\vec{g}^T x_{s-1})\sigma^2. \quad (29)$$

It is apparent from (27), (28) and (29), that the desired signal component s_s and the statistics of the noise contribution z_s of the decision variable y_s are determined by the present symbol x_s and the most recent past symbol x_{s-1}. Hence, we can implement the MLSE as a simple two-state Viterbi

algorithm:

$$\operatorname*{argmax}_{\hat{\vec{x}}} \log \left\{ p\left(\vec{y}|\hat{\vec{x}}, \mathcal{C}_i\right) \right\}$$

$$= \operatorname*{argmin}_{\hat{\vec{x}}} \sum_{s=1}^{2K+1} \frac{|y_s - s_s - \overline{z}_s|^2}{2\sigma_{z,s}^2} + 0.5 \log\left(2\pi\sigma_{z,s}^2\right)$$

$$= \operatorname*{argmin}_{\hat{\vec{x}}} \sum_{s=1}^{2K+1} m(y_s, \hat{x}_s, \zeta_s), \qquad (30)$$

with ζ_s, the state of the Viterbi algorithm at time instance s.

V. PERFORMANCE RESULTS

To see the impact of the CSI, we compare the performance of the above derived ML receivers and the MLSE by means of bit error rate (BER) simulations. The BER is plotted over the signal-to-noise ratio E_b/N_0, where E_b denotes the energy per bit and $N_0/2$ is the noise power spectral density. We assume uniformly distributed channel taps within the duration of the channel impulse response. To achieve a data rate of 50 Mbps with 2PPM, one bit has to be transmitted every 20 ns. Hence, one PPM frame has a duration of $T = 20$ ns, i.e., one PPM slot has a duration of 10 ns and ISI occurs for channel impulse responses with a duration of more than 10 ns. We consider the cases that no ISI, weak ISI, and strong ISI occurs. In case of no ISI the CIR has a duration of 10 ns, in case of weak ISI 14 ns, and in case of strong ISI 17 ns.

a) No ISI: The BER curves in case of no ISI are shown in Fig. 2. As expected, the higher the amount of CSI the better is the performance of the corresponding receiver. However, this performance improvement is achieved at the cost of a higher receiver complexity. The ML$_{\text{full}}$, which does a coherent combining, performs best and meets the matched filter (MF) bound. Since the ML$_{\text{IPDP}}$ has no information on the signs of the channel taps, no coherent combining is possible. The performance of this receiver structure is about 5 dB worse compared to the MF. A further performance degradation of about 2 dB is observed for the ML$_{\text{APDP}}$. Then, the channel taps cannot be weighted with the instantaneous power but only with the average power. Since we assume uniformly distributed channel taps and a CIR duration of 10 ns, the ML$_{\text{APDP}}$ equals in this case the energy detector. Therefore, the performance of these both receivers is the same. In absence of ISI, the MLSE corresponds to a symbol-wise energy detector and thus the performance of the MLSE and the energy detector are the same, too.

b) Weak ISI: The performance of the ML receivers not considering the ISI becomes worse in the presence of ISI as it can be seen in Fig. 3. As expected, the performance improves if the ML receivers are adapted to the ISI. The ML$_{\text{full}}$ is about 2 dB worse compared with the no ISI case. However, the MML$_{\text{full,ISI}}$ loses only about 0.8 dB. A similar observation can be made for the ML receivers with IPDP. While the ML$_{\text{IPDP}}$ degrades by about 4 dB, the ML$_{\text{IPDP,ISI}}$ is only about 1.5 dB worse compared to the result in Fig. 2.
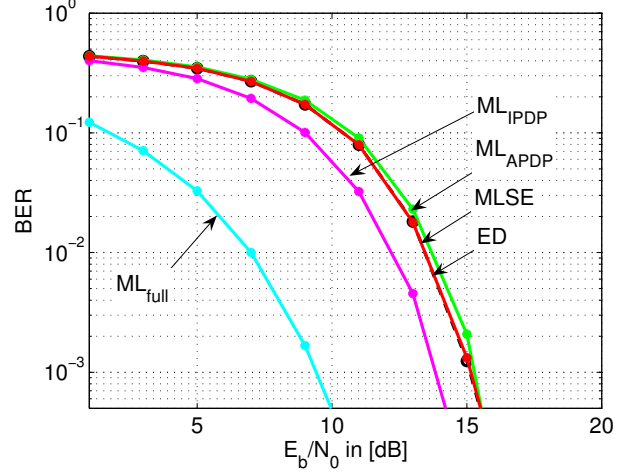

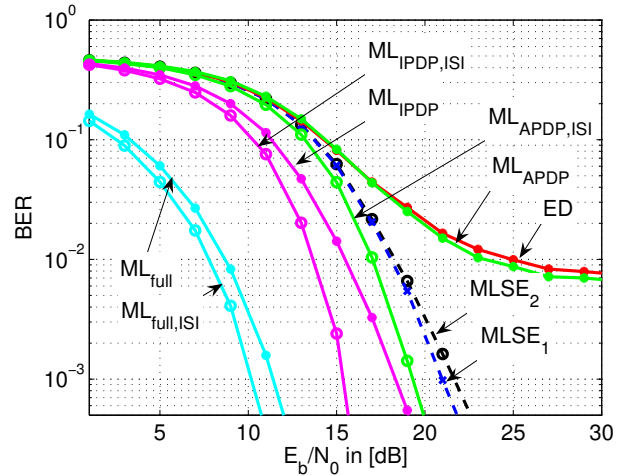Fig. 2.   Bit error rate curves in the case of no ISI

Fig. 3.   Bit error rate curves in the case of weak ISI

Therefore, the MLs with full CSI and IPDP do not necessarily have to be optimized for ISI if only weak ISI is present. For the ML$_{\text{APDP}}$ and for the energy detector a different behavior can be observed. Due to the ISI, the influence of the noise on the BER performance is not dominant for high E_b/N_0 values and the BER curves approach an error floor. The ML$_{\text{APDP,ISI}}$ shows a much better performance and is about 4 dB worse compared to the no ISI case. Although the receiver complexity for the ML$_{\text{APDP,ISI}}$ is somewhat higher than for the ML$_{\text{APDP}}$, the ML$_{\text{APDP,ISI}}$ should be used in case of ISI due to the much better performance. Both MLSE show almost the same performance and are about 1.5 dB worse than the symbol-wise ML receiver with APDP. The simpler MLSE, which neglects the cross-correlation terms, is only about 0.5 dB worse than the one considering those terms because neglecting the cross-correlation terms does not influence the performance in the plotted E_b/N_0 range too much.
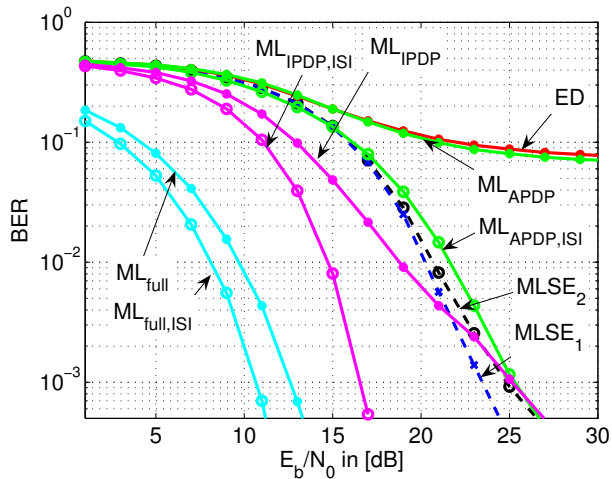
Fig. 4.   Bit error rate curves in the case of strong ISI

c) Strong ISI: The BER curves for strong ISI are plotted in Fig. 4. As above, we also compare the ML receivers that are adapted to the ISI with the ones that are optimized for no ISI. The ML receivers not optimized for ISI perform in the strong ISI scenario much worse than in the weak ISI scenario except for the ML_{full}. The performance of the ML_{full} degrades only slightly while the energy detector and the ML_{APDP} exhibit an error floor at about $8 \cdot 10^{-2}$. An error floor for high E_b/N_0 values can also be expected for the ML_{IPDP}. The ML receivers that consider ISI show a much better performance. The $ML_{full,ISI}$ is only about 1.6 dB, the $ML_{IPDP,ISI}$ about 2.6 dB, and the $ML_{APDP,ISI}$ about 6 dB worse than the corresponding "no ISI" BER curves at a BER $= 10^{-3}$. In contrast to the weak ISI scenario, the MLSE perform here better than the $ML_{APDP,ISI}$. Nevertheless, both MLSE lose about 2 dB when having strong ISI instead of weak ISI. Although the performance of both MLSE and the $ML_{APDP,ISI}$ is worse compared to the $ML_{full,ISI}$ and the $ML_{IPDP,ISI}$, they are very attractive for the use in BAN due to their lower complexity. For the $ML_{full,ISI}$ and the $ML_{IPDP,ISI}$ a precise channel estimation is necessary which increases the receiver complexity. Hence, these both structures are rather suited for applications with relaxed complexity constraints or very high data rates where strong ISI occurs.

VI. Conclusions

We presented a family of symbol-wise detectors for 2PPM, which utilize partial channel state information to improve the robustness to ISI. We considered the cases of no CSI, APDP, IPDP, and full CSI. In the presence of ISI, the performance of the ML receivers that are not adapted to ISI degraded and approached an error floor for high signal-to-noise ratios. If the ISI is considered by the ML, the performance could be improved substantially. However, from the equations and the

BER curves a tradeoff between complexity and performance could be observed. The performance becomes better with increasing amount of CSI and consideration of the ISI but results in a much higher receiver complexity. Moreover, the ML receivers with partial CSI require an estimation of the CSI, which increases the complexity even more. Hence, we presented also two simple post-detection MLSE receivers that base their decision on the output of an energy detector. These MLSE receivers showed almost the same performance as the symbol-wise ML with APDP requiring a less complex receiver structure and very small CSI that can be easily obtained. Hence, for a very simple UWB BAN, the MLSE receivers are most promising although the performance is worse compared to the cases with full CSI and IPDP.

References

[1] T. Zasowski, F. Althaus, M. Stäger, A. Wittneben, and G. Tröster, "UWB for noninvasive wireless body area networks: Channel measurements and results," *IEEE UWBST 2003*, pp. 285–289, November 2003.

[2] S. Jung, C. Lauterbach, M. Strasser, and W. Weber, "Enabling technologies for disappearing electronics in smart textiles," *2003 IEEE ISSCC*, vol. 1, pp. 386–387, February 2003.

[3] T. Zasowski, G. Meyer, F. Althaus, and A. Wittneben, "UWB signal propagation at the human head," *IEEE Trans. on MTT*, vol. 54, no. 4, April 2006.

[4] C. Carbonelli and U. Mengali, "Low complexity synchronization for UWB noncoherent receivers," *IEEE VTC 2005 Spring*, pp. 379–384, September 2005.

[5] M. Weisenhorn and W. Hirt, "ML receiver for pulsed UWB signals and parital channel state information," *IEEE ICU 2005*, pp. 379–384, September 2005.

[6] H. Celebi and H. Arslan, "Cross-modulation interference for pulse position modulated UWB signals," *IEEE MILCOM 2005*, pp. 1–7, October 2005.

[7] T. Zasowski and A. Wittneben, "UWB transmitted reference receivers in the presence of co-channel interference," *IEEE PIMRC 2006*, September 2006.

[8] A. Papoulis and S. U. Pillai, *Probability, Random Variables and Stochastic Processes*, 4th ed.   McGraw-Hill Higher Education, 2002.

[9] M. Weisenhorn and W. Hirt, "Robust noncoherent receiver exploiting UWB channel properties," *Joint UWBST & IWUWBS 2004*, May 2004.

[10] J. R. Barry, "Sequence detection and equalization for pulse-position modulation," in *Proc. ICC*, New Orleans, LA, US, 1–5 May 1994.

[11] A. Klein and J. Johnson, C.R., "MMSE Decision Feedback Equalization of Pulse Position Modulated Signals," in *Proc. ICC*, Ithaca, NY, US, 20–24 June 2004.

[12] M. Sahin and H. Arslan, "Inter-symbol interference in high data rate UWB communications using energy detector receivers," in *IEEE Int. Conf. Ultra-Wideband (ICU)*, Zurich, Switzerland, Sept. 5 – 8, 2005.

[13] A. R. Forouzan and M. Abtahi, "Application of convolutional error correcting codes in ultrawideband M-ary PPM signaling," *IEEE Microwave and Wireless Components Letter*, vol. 13, no. 8, pp. 308 – 310, Aug. 2003.

[14] G. D. Forney, "Maximum-likelihood sequence estimation in the presence of intersymbol interference," *IEEE Trans. Inform. Theory*, vol. 18, no. 3, pp. 363–378, May 1972.

[15] S. Dubouloz, B. Denis, S. De Rivaz, and O. Laurent, "Performance analysis of LDR UWB non-coherent receivers in multipath environments," in *IEEE Int. Conf. Ultra-Wideband (ICU)*, Zurich, Switzerland, Sept. 5 – 8, 2005, pp. 491–496.

[16] F. Troesch, F. Althaus, and A. Wittneben, "Modified pulse repetition coding boosting energy detector performance in low data rate systems," in *IEEE Int. Conf. Ultra-Wideband (ICU)*, Zurich, Switzerland, Sept. 5 – 8, 2005.